

Resonance fluorescence of a two-level atom in a two-mode squeezed vacuum

A. S. Parkins

Department of Physics, University of Waikato, Hamilton, New Zealand

(Received 9 July 1990)

The dynamics of a strongly driven two-level atom are examined for the case that the atom is coupled to a "two-mode" squeezed vacuum. The source of squeezed light is taken to be a (frequency) nondegenerate parametric oscillator. We consider the situation in which the Rabi sidebands produced by the coherent driving field coincide with the spectral peaks of the parametric oscillator. Approximate analytical results are presented and checked against numerical simulations of the exact equations. For a suitable choice of relative phase, all three spectral lines in the fluorescence triplet are found to exhibit subnatural linewidths. Significant modifications to the fluorescence spectrum are also possible with a nonzero laser-atom detuning.

I. INTRODUCTION

In a recent work examining resonance fluorescence of a single strongly driven two-level atom coupled to a *narrow* bandwidth squeezed vacuum,¹ we found significant departures from broadband (or white-noise) squeezed-vacuum analyses.² The white-noise formulation assumes that the squeezed vacuum appears δ correlated on the time scale of the Rabi oscillations. This corresponds to a squeezing bandwidth much larger than the Rabi frequency. Under these conditions the central peak in the fluorescence triplet is found to exhibit a subnatural or supernatural linewidth, depending on the relative phase between the driving field and the squeezed vacuum, while the Rabi sidebands are broadened for all choices of the relative phase.

A small-noise (linearized) analysis of the Bloch equations reveals that the Rabi frequency Ω_0 provides a means of controlling which reservoir spectral components contribute to Bloch-vector damping.³ In particular, the decay rates of the Bloch-vector components are determined by fluctuations in one quadrature phase of the input field at frequency ω_0 and in the other quadrature phase at frequencies $\omega_0 \pm \Omega_0$,¹ where ω_0 is the frequency of the coherent driving field (resonant with the transition frequency). In the white-noise model, these observations have little significance, as the level of fluctuations in both quadratures is constant over the entire frequency space.

However, if the squeezing bandwidth is taken, as in Ref. 1, to be much *smaller* than the Rabi frequency, then the quadratures exhibit enhanced or reduced fluctuations only in a relatively narrow frequency band about ω_0 , outside of which ordinary vacuum fluctuations predominate. Hence the narrow-bandwidth component of one quadrature is effectively decoupled from the atomic dynamics, leading to dramatic changes from the white-noise theory. The central fluorescence peak is now virtually unaffected by the squeezed vacuum, retaining its normal-vacuum profile independent of the choice of phase. However, the

width of the Rabi sidebands is strongly phase dependent and can be significantly less than its normal-vacuum width. Hence a finite-bandwidth squeezed vacuum offers new possibilities for line narrowing in the fluorescence spectrum.

An interesting variation on this theme, which we shall pursue here, is a "two-mode" squeezed vacuum exhibiting two (separated) spectral peaks centered on the frequencies $\omega_0 \pm \Omega_0$. Once again it should be possible to decouple the narrow-bandwidth component of one quadrature from the dynamics. This is not merely a construction of convenience either, since squeezing spectra with this double-peaked form are found in the output of a number of practical squeezing devices. The particular source we shall employ in this work is the nondegenerate parametric oscillator operating below threshold,^{4,5} but similar spectra are also found, for example, in optical bistability.⁶

In Sec. II we formulate our description of the system and of the squeezed light source. In Sec. III A we present an approximate analytical treatment of the Bloch equations that highlights the basic features of the scheme. This also provides a benchmark for the results we obtain later in Sec. III B from direct stochastic simulation of the exact equations. As we shall see, the present scheme shows features characteristic of both the "single-mode" white-noise and colored-noise results. It differs in a significant way, however, in that it offers the possibility of simultaneous narrowing of all three components of the fluorescence triplet, a feature not found in any of the previous treatments.

II. MODEL

A. Quantum Langevin equations and the adjoint equation

Our approach to this problem begins with the quantum Langevin equations for the familiar (two-level) atomic system operators S^+ and S_z . This approach is outlined in Ref. 7 and is the same as that used by us in Ref. 1. The equations are

$$\begin{aligned}\dot{S}^+ &= i\omega_a S^+ - i\Omega_0 \cos(\omega_0 t - \phi_0) S_z \\ &\quad - \frac{i}{2} \sqrt{\gamma_a / \hbar \omega_a} [E_{\text{in}}(t), S_z]_+, \\ \dot{S}_z &= -\gamma_a - 2i\Omega_0 \cos(\omega_0 t - \phi_0) (S^+ - S^-) \\ &\quad - i\sqrt{\gamma_a / \hbar \omega_a} [E_{\text{in}}(t), S^+ - S^-]_+, \end{aligned} \quad (2.1)$$

where ω_a is the atomic transition frequency, γ_a is the natural linewidth of the transition, and Ω_0 and ϕ_0 are the Rabi frequency and phase, respectively, of the coherent driving field. The incoming electric-field operator $E_{\text{in}}(t)$ (representing the incoherent portion of the field) is evaluated at the position of the atom and may be expressed in terms of quadrature phase operators as

$$\begin{aligned}E_{\text{in}}(t) &= \sqrt{\hbar \omega_0} [a_{\text{in}}(t) e^{-i\omega_0 t} + a_{\text{in}}^\dagger(t) e^{i\omega_0 t}] \\ &= \sqrt{\hbar \omega_0} [E_1(t) \cos(\omega_0 t) + E_2(t) \sin(\omega_0 t)], \end{aligned} \quad (2.2)$$

where ω_0 is the frequency of the coherent driving field.

We move to a frame rotating at frequency ω_0 and define polarization quadratures that are in-phase and out-of-phase with the coherent driving field:

$$\begin{aligned}S_x &= S^+ \exp(-i\omega_0 t + i\phi_0) + S^- \exp(i\omega_0 t - i\phi_0), \\ S_y &= -i[S^+ \exp(-i\omega_0 t + i\phi_0) - S^- \exp(i\omega_0 t - i\phi_0)]. \end{aligned} \quad (2.3)$$

We make the rotating wave approximation to produce equations of motion in the form

$$\begin{aligned}\dot{S}_x &= -\Delta_a S_y + \frac{1}{2} \sqrt{\gamma_a} [E_1(t) \sin(\phi_0) - E_2(t) \cos(\phi_0), S_z]_+, \\ \dot{S}_y &= \Delta_a S_x - \Omega_0 S_z - \frac{1}{2} \sqrt{\gamma_a} [E_1(t) \cos(\phi_0) \\ &\quad + E_2(t) \sin(\phi_0), S_z]_+, \\ \dot{S}_z &= -\gamma_a + \Omega_0 S_y + \frac{1}{2} \sqrt{\gamma_a} [E_1(t) \cos(\phi_0) \\ &\quad + E_2(t) \sin(\phi_0), S_y]_+ \\ &\quad - \frac{1}{2} \sqrt{\gamma_a} [E_1(t) \sin(\phi_0) - E_2(t) \cos(\phi_0), S_x]_+, \end{aligned} \quad (2.4)$$

where $\Delta_a = \omega_a - \omega_0$. At this point we introduce the adjoint equation. This equation (whose derivation from the quantum Langevin equation is given in Ref. 7) describes the time evolution of a quantity $\mu(t)$ which is a 2×2 matrix functional of the incoming electric-field operator $E_{\text{in}}(t)$. We define

$$\bar{S}_i(t) \equiv \text{Tr}_{\text{sys}} [S_i \mu(t)], \quad (2.5)$$

as the *atomic* average of the spin operators, and the equations that follow have the form

$$\begin{aligned}\dot{\bar{S}}_x &= -\Delta_a \bar{S}_y - \beta_X(t) \bar{S}_z, \\ \dot{\bar{S}}_y &= \Delta_a \bar{S}_x - \Omega_0 \bar{S}_z - \beta_Y(t) \bar{S}_z, \\ \dot{\bar{S}}_z &= -\gamma_a + \Omega_0 \bar{S}_y + \beta_X(t) \bar{S}_x + \beta_Y(t) \bar{S}_y, \end{aligned} \quad (2.6)$$

where $\beta_X(t)$ and $\beta_Y(t)$ are defined by

$$\begin{aligned}\beta_X(t) \rho &= \frac{1}{2} \sqrt{\gamma_a} \{-\sin(\phi_0) [E_1(t), \rho]_+ + \cos(\phi_0) [E_2(t), \rho]_+\} \\ &\equiv [-\sin(\phi_0) \beta_1(t) + \cos(\phi_0) \beta_2(t)] \rho, \\ \beta_Y(t) \rho &= \frac{1}{2} \sqrt{\gamma_a} \{\cos(\phi_0) [E_1(t), \rho]_+ + \sin(\phi_0) [E_2(t), \rho]_+\} \\ &\equiv [\cos(\phi_0) \beta_1(t) + \sin(\phi_0) \beta_2(t)] \rho. \end{aligned} \quad (2.7)$$

The point in making these definitions is that we now have a commuting form of quantum noise; that is, the operators $\beta_X(t)$ and $\beta_Y(t)$ satisfy

$$\begin{aligned}[\beta_X(t), \beta_X(t')] &= [\beta_Y(t), \beta_Y(t')] \\ &= [\beta_X(t), \beta_Y(t')] = 0, \end{aligned} \quad (2.8)$$

for all t, t' . This implies that the equations can be treated as classical *c*-number equations, amenable to solution by ordinary stochastic methods. Hence we need only specify the statistics of $\beta_X(t)$ and $\beta_Y(t)$, as determined by the initial quantum state of the incoming electric field (the bath).

B. Two-mode squeezing: The nondegenerate parametric oscillator

Our source of squeezed light is taken to be a nondegenerate parametric amplifier operating (below threshold) in a single-ended cavity. In this configuration, a pump beam at frequency $2\omega_0$ is coupled, via a nonlinear medium, to two cavity modes at frequencies $\omega_0 \pm \delta_c = \omega_\pm$. The two modes excited in this way may become highly correlated, leading to squeezed-frequency components in two (separated) spectral peaks, centered, respectively, at the mode frequencies ω_+ and ω_- .

The correlation functions for the output-mode operators of the nondegenerate parametric oscillator operating below threshold (with a classical pump) have been given by Collett, Loudon, and Gardiner.⁴ We consider, of course, the case in which the signal and idler components are combined in a single beam. With a particular choice of phase that makes the parametric driving rate ϵ_c real [$\theta = 0$ in Eqs. (A18) and (A19) of Ref. 4], these correlation functions have the form (in a frame rotating at frequency ω_0)

$$\begin{aligned}\langle a_{\text{in}}^\dagger(t) a_{\text{in}}(t') \rangle &= \frac{1}{4} \epsilon_c \gamma_c \exp(-\frac{1}{2} \gamma_c |t - t'|) \\ &\quad \times \left[\frac{\exp(\frac{1}{2} \epsilon_c |t - t'|)}{\frac{1}{2} \gamma_c - \frac{1}{2} \epsilon_c} - \frac{\exp(-\frac{1}{2} \epsilon_c |t - t'|)}{\frac{1}{2} \gamma_c + \frac{1}{2} \epsilon_c} \right] \\ &\quad \times \cos[\delta_c(t - t')], \\ \langle a_{\text{in}}(t) a_{\text{in}}(t') \rangle &= -\frac{1}{4} \epsilon_c \gamma_c \exp(-\frac{1}{2} \gamma_c |t - t'|) \\ &\quad \times \left[\frac{\exp(\frac{1}{2} \epsilon_c |t - t'|)}{\frac{1}{2} \gamma_c - \frac{1}{2} \epsilon_c} + \frac{\exp(-\frac{1}{2} \epsilon_c |t - t'|)}{\frac{1}{2} \gamma_c + \frac{1}{2} \epsilon_c} \right] \\ &\quad \times \cos[\delta_c(t - t')], \end{aligned} \quad (2.9)$$

where $\gamma_c/2$ is the cavity-mode decay rate (the same for both modes), and the results are derived with the assumption that $\omega_+ - \omega_- = 2\delta_c \gg \gamma_c$. Note that we have removed a factor of $\frac{1}{2}$ from ϵ_c as defined in Ref. 4. In the limit of perfect squeezing, $\epsilon_c \rightarrow \gamma_c$. No loss of generality occurs by fixing the phase of the input squeezed vacuum. What is important is the relative phase between the squeezed vacuum and the coherent driving field, and obviously, this can be controlled through the phase of the coherent field ϕ_0 .

$$\begin{aligned}
\langle \beta_1(t)\beta_1(t') \rangle &= \gamma_a \langle E_1(t)E_1(t') \rangle \\
&= \gamma_a \left[-\frac{\epsilon_c \gamma_c}{\frac{1}{2}\gamma_c + \frac{1}{2}\epsilon_c} \exp[-\frac{1}{2}(\gamma_c + \epsilon_c)|t-t'|] \cos[\delta_c(t-t')] + \delta(t-t') \right], \\
\langle \beta_2(t)\beta_2(t') \rangle &= \gamma_a \langle E_2(t)E_2(t') \rangle \\
&= \gamma_a \left[\frac{\epsilon_c \gamma_c}{\frac{1}{2}\gamma_c - \frac{1}{2}\epsilon_c} \exp[-\frac{1}{2}(\gamma_c - \epsilon_c)|t-t'|] \cos[\delta_c(t-t')] + \delta(t-t') \right], \\
\langle \beta_1(t)\beta_2(t') \rangle &= 0.
\end{aligned} \tag{2.10}$$

Hence $\beta_1(t)$ exhibits reduced fluctuations in two spectral peaks centered at frequencies $\pm\delta_c$ and with linewidth $\frac{1}{2}(\gamma_c + \epsilon_c)$, while $\beta_2(t)$ exhibits enhanced fluctuations in two spectral peaks of linewidth $\frac{1}{2}(\gamma_c - \epsilon_c)$.

III. SOLUTIONS TO THE EQUATIONS OF MOTION

As a preliminary step, we express each of the noise sources as a sum of independent colored- and white-noise sources. For instance, we write

$$\beta_1(t) = \beta_1^c(t) + \beta_1^w(t), \tag{3.1}$$

where

$$\begin{aligned}
\langle \beta_1^w(t)\beta_1^w(t') \rangle &= \gamma_a \delta(t-t'), \\
\langle \beta_1^c(t)\beta_1^c(t') \rangle &= -\gamma_a \frac{\epsilon_c \gamma_c}{\frac{1}{2}\gamma_c + \frac{1}{2}\epsilon_c} \exp[-\frac{1}{2}(\gamma_c + \epsilon_c)|t-t'|] \\
&\quad \times \cos[\delta_c(t-t')].
\end{aligned} \tag{3.2}$$

We then perform a straightforward average over the white-noise sources to yield equations in the form

$$\begin{aligned}
\dot{\bar{S}}_x &= -\frac{\gamma_a}{2} \bar{S}_x - \Delta_a \bar{S}_y - \beta_X^c(t) \bar{S}_z, \\
\dot{\bar{S}}_y &= -\frac{\gamma_a}{2} \bar{S}_y + \Delta_a \bar{S}_x - \Omega_0 \bar{S}_z - \beta_Y^c(t) \bar{S}_z, \\
\dot{\bar{S}}_z &= -\gamma_a - \gamma_a \bar{S}_z + \Omega_0 \bar{S}_y + \beta_X^c(t) \bar{S}_x + \beta_Y^c(t) \bar{S}_y,
\end{aligned} \tag{3.3}$$

In specifying the correlation functions of the input field operators to be given by (2.9), we are of course assuming that the atom couples only to squeezed modes of the radiation field. This is a very difficult practical requirement which we shall return to in the conclusion.

Using (2.9) and the definitions (2.2) and (2.4), it is then straightforward to determine the correlation functions of the noise sources $\beta_1(t)$ and $\beta_2(t)$ appearing in the equations of motion. These are

where the bar is now understood to incorporate the white-noise average. It remains therefore to perform the average over $\beta_X^c(t)$ and $\beta_Y^c(t)$ to obtain $\langle S_i(t) \rangle$, where $\langle \rangle$ denotes the total average.

In view of the somewhat unusual spectrum of noise exhibited by $\beta_X^c(t)$ and $\beta_Y^c(t)$ (spectral peaks at frequencies $\pm\delta_c$), it is a good idea first to perform a qualitative inspection of Eqs. (3.3), in order to identify the most interesting regions of parameter space.

In the lowest order (neglecting noise terms) and for zero detuning, $\langle S_x(t) \rangle$ displays a simple exponential decay, while $\langle S_y(t) \rangle$ and $\langle S_z(t) \rangle$ exhibit damped oscillations of frequency Ω_0 . The contribution to the time development of $\langle S_x(t) \rangle$ from the additional noise terms is proportional to the time average of $\beta_X^c(t) \bar{S}_z(t)$. Since $\bar{S}_z(t)$ undergoes Rabi oscillations, it follows that this contribution will be important only if $\beta_X^c(t)$ contains significant Fourier components at the frequencies $\pm\Omega_0$. In our instance, this clearly corresponds to the case in which $\delta_c \simeq \Omega_0$. In contrast, the contribution of the terms $\beta_Y^c(t) \bar{S}_z(t)$ and $\beta_Y^c(t) \bar{S}_y(t)$ to the overall evolution will be significant only if $\beta_Y^c(t)$ possesses Fourier components around zero frequency. This is clearly *not* the case for the “two-mode” squeezed vacuum we are modeling here. Hence we expect that $\beta_Y^c(t)$ can be effectively decoupled from the atomic dynamics for sufficiently large Ω_0 and δ_c . As pointed out in Ref. 1, this has special significance in the case of a squeezed-vacuum input, since through an appropriate choice of the phase ϕ_0 , $\beta_Y^c(t)$ can be made to correspond to the unsqueezed (noisy) quadrature.

The important difference between the present “two-mode” formulation and the “single-mode” squeezed-vacuum model examined in Ref. 1 is that a different quadrature phase noise operator is decoupled. In the

“single-mode” model, $\beta_x^c(t)$ and $\beta_y^c(t)$ have Fourier components only in a relatively small frequency band around zero frequency, and hence $\beta_x^c(t)$ is decoupled from the equations of motion. Of course, in the “single-mode” white-noise model,² neither quadrature phase noise operator can be decoupled as their Fourier components are significant over the whole of frequency space.

A. Decorrelation approximation

We begin with an approximate analytical solution to the equations of motion which relies on the assumption that the noise sources and system variables can be decorrelated under averaging. Briefly, we solve formally for two of the system variables and substitute the results into the equation of motion for the third variable, after which averaging is performed in the decorrelation approximation. Two distinct limiting cases characterize our problem, corresponding to the choices of phase $\phi_0=0$ and $\pi/2$. For simplicity, we shall consider only these two cases, and hence we write

$$\begin{aligned} \langle \dot{S}_x(t) \rangle &= -\frac{\gamma_a}{2} \langle S_x(t) \rangle \\ &+ \frac{\gamma_a^2}{2\Omega_0} (N \pm M) b_{\pm} \int_0^t dt' \exp \left[-\left[\frac{3\gamma_a}{4} + b_{\pm} \right] (t-t') \right] \sin[\Omega_0(t-t')] \cos[\delta_c(t-t')] \langle S_x(t') \rangle \\ &- 2\gamma_a (N \pm M) b_{\pm} \int_0^t dt' \exp \left[-\left[\frac{3\gamma_a}{4} + b_{\pm} \right] (t-t') \right] \cos[\Omega_0(t-t')] \cos[\delta_c(t-t')] \langle S_x(t') \rangle, \end{aligned} \quad (3.6a)$$

$$\begin{aligned} \langle \dot{S}_y(t) \rangle &= -\frac{\gamma_a}{2} \langle S_y(t) \rangle - \Omega_0 \langle S_z(t) \rangle \\ &+ \frac{\gamma_a^2}{2\Omega_0} (N \mp M) b_{\mp} \int_0^t dt' \exp \left[-\left[\frac{3\gamma_a}{4} + b_{\mp} \right] (t-t') \right] \sin[\Omega_0(t-t')] \cos[\delta_c(t-t')] \langle S_y(t') \rangle \\ &- 2\gamma_a (N \mp M) b_{\mp} \int_0^t dt' \exp \left[-\left[\frac{3\gamma_a}{4} + b_{\mp} \right] (t-t') \right] \cos[\Omega_0(t-t')] \cos[\delta_c(t-t')] \langle S_y(t') \rangle \\ &+ 2\gamma_a (N \mp M) b_{\mp} \int_0^t dt' \exp \left[-\left[\frac{3\gamma_a}{4} + b_{\mp} \right] (t-t') \right] \sin[\Omega_0(t-t')] \cos[\delta_c(t-t')] \langle S_z(t') \rangle, \end{aligned} \quad (3.6b)$$

$$\begin{aligned} \langle \dot{S}_z(t) \rangle &= -\gamma_a - \gamma_a \langle S_z(t) \rangle + \Omega_0 \langle S_y(t) \rangle - 2\gamma_a (N \pm M) b_{\pm} \int_0^t dt' \exp \left[-\left[\frac{\gamma_a}{2} + b_{\pm} \right] (t-t') \right] \cos[\delta_c(t-t')] \langle S_z(t') \rangle \\ &- \frac{\gamma_a^2}{2\Omega_0} (N \mp M) b_{\mp} \int_0^t dt' \exp \left[-\left[\frac{3\gamma_a}{4} + b_{\mp} \right] (t-t') \right] \sin[\Omega_0(t-t')] \cos[\delta_c(t-t')] \langle S_z(t') \rangle \\ &- 2\gamma_a (N \mp M) b_{\mp} \int_0^t dt' \exp \left[-\left[\frac{3\gamma_a}{4} + b_{\mp} \right] (t-t') \right] \cos[\Omega_0(t-t')] \cos[\delta_c(t-t')] \langle S_z(t') \rangle \\ &- 2\gamma_a (N \mp M) b_{\mp} \int_0^t dt' \exp \left[-\left[\frac{3\gamma_a}{4} + b_{\mp} \right] (t-t') \right] \sin[\Omega_0(t-t')] \cos[\delta_c(t-t')] \langle S_y(t') \rangle. \end{aligned} \quad (3.6c)$$

As mentioned earlier, we expect the most interesting results when δ_c and Ω_0 are comparable, and so for simplicity we choose $\delta_c = \Omega_0$. We know further that $\delta_c \gg b_{\pm}$. If b_+ and b_- are larger than the decay rates of the various spin components, then to a good approximation we can make the following substitutions inside the integrals:

$$\begin{aligned} \langle \beta_x^c(t) \beta_x^c(t') \rangle &= 2\gamma_a (N \pm M) b_{\pm} e^{-b_{\pm}|t-t'|} \\ &\quad \times \cos[\delta_c(t-t')], \\ \langle \beta_y^c(t) \beta_y^c(t') \rangle &= 2\gamma_a (N \mp M) b_{\mp} e^{-b_{\mp}|t-t'|} \\ &\quad \times \cos[\delta_c(t-t')], \\ \langle \beta_x^c(t) \beta_y^c(t') \rangle &= 0, \end{aligned} \quad (3.4)$$

where $b_+ = \frac{1}{2}(\gamma_c - \epsilon_c)$ and $b_- = \frac{1}{2}(\gamma_c + \epsilon_c)$, and we have introduced the familiar squeezing parameters N and M , defined by

$$\begin{aligned} N + M &= \frac{\frac{1}{2}\epsilon_c \gamma_c}{(\frac{1}{2}\gamma_c - \frac{1}{2}\epsilon_c)^2}, \\ N - M &= -\frac{\frac{1}{2}\epsilon_c \gamma_c}{(\frac{1}{2}\gamma_c + \frac{1}{2}\epsilon_c)^2}. \end{aligned} \quad (3.5)$$

The limit of large squeezing ($\epsilon_c \rightarrow \gamma_c$) corresponds to the limit $N \gg 1$. We assume a strong driving field ($\Omega_0 \gg \gamma_a$) and set $\Delta_a = 0$. We find, after some work,

$$\begin{aligned}
\langle S_x(t') \rangle &\approx \langle S_x(t) \rangle, \\
\langle S_y(t') \rangle &\approx \cos[\Omega_0(t-t')] \langle S_y(t) \rangle + \sin[\Omega_0(t-t')] \langle S_z(t) \rangle, \\
\langle S_z(t') \rangle &\approx \cos[\Omega_0(t-t')] \langle S_z(t) \rangle - \sin[\Omega_0(t-t')] \langle S_y(t) \rangle.
\end{aligned} \tag{3.7}$$

The assumption of large b_{\pm} restricts the maximum amount of squeezing we can consider for a particular value of γ_c , since $b_{\pm} \rightarrow 0$ in the large squeezing limit. However, this maximum amount of squeezing can always be increased via an increase in γ_c .

With the substitutions given in (3.7), we have simply to evaluate some straightforward integrals. This produces time-dependent terms, but with the assumptions made above, these are expected to give only small transient effects and so we neglect them. The result of these approximations is a set of modified Bloch equations with the form

$$\begin{aligned}
\langle \dot{S}_x \rangle &\simeq -\gamma_x \langle S_x \rangle, \\
\langle \dot{S}_y \rangle &\simeq -\gamma_y \langle S_y \rangle - \Omega_z \langle S_z \rangle, \\
\langle \dot{S}_z \rangle &\simeq -\gamma_a - \gamma_z \langle S_z \rangle + \Omega_y \langle S_y \rangle,
\end{aligned} \tag{3.8}$$

where

$$\begin{aligned}
\gamma_x &= \frac{\gamma_a}{2} \left[1 + 2(N \pm M) b_{\pm} \left[\frac{1}{b_{\pm} + 3\gamma_a/4} + \frac{b_{\pm} + \gamma_a/4}{(b_{\pm} + 3\gamma_a/4)^2 + 4\Omega_0^2} \right] \right], \\
\gamma_y &= \frac{\gamma_a}{2} \left[1 + 2(N \mp M) b_{\mp} \left[\frac{b_{\mp} + 11\gamma_a/8}{(b_{\mp} + 3\gamma_a/4)^2 + \Omega_0^2} - \frac{3\gamma_a/8}{(b_{\mp} + 3\gamma_a/4)^2 + 9\Omega_0^2} \right] \right], \\
\gamma_z &= \gamma_a \left[1 + (N \pm M) \frac{b_{\pm}}{b_{\pm} + \gamma_a/2} + (N \pm M) \frac{b_{\pm}(b_{\pm} + \gamma_a/2)}{(b_{\pm} + \gamma_a/2)^2 + 4\Omega_0^2} \right. \\
&\quad \left. + 2(N \mp M) \frac{b_{\mp}(b_{\mp} + 3\gamma_a/4)}{(b_{\mp} + 3\gamma_a/4)^2 + \Omega_0^2} + \frac{1}{8}(N \mp M) \left[\frac{\gamma_a b_{\mp}}{(b_{\mp} + 3\gamma_a/4)^2 + \Omega_0^2} + \frac{3\gamma_a b_{\mp}}{(b_{\mp} + 3\gamma_a/4)^2 + 9\Omega_0^2} \right] \right],
\end{aligned} \tag{3.9}$$

and

$$\begin{aligned}
\Omega_z &= \Omega_0 \left[1 - \frac{\gamma_a^2}{8\Omega_0^2} (N \mp M) b_{\mp} \left[\frac{b_{\mp} + 3\gamma_a/4}{(b_{\mp} + 3\gamma_a/4)^2 + \Omega_0^2} - \frac{b_{\mp} + 3\gamma_a/4}{(b_{\mp} + 3\gamma_a/4)^2 + 9\Omega_0^2} \right] \right], \\
\Omega_y &= \Omega_0 \left[1 + \frac{\gamma_a^2}{8\Omega_0^2} (N \mp M) b_{\mp} \left[\frac{b_{\mp} + 3\gamma_a/4}{(b_{\mp} + 3\gamma_a/4)^2 + \Omega_0^2} - \frac{b_{\mp} + 3\gamma_a/4}{(b_{\mp} + 3\gamma_a/4)^2 + 9\Omega_0^2} \right] + 2\gamma_a (N \pm M) \frac{b_{\pm}}{(b_{\pm} + \gamma_a/2)^2 + 4\Omega_0^2} \right].
\end{aligned} \tag{3.10}$$

The limit we are considering ($\Omega_0 \gg b_{\pm}, \gamma_x, \gamma_y, \gamma_z$) allows for considerable simplification of (3.9) and (3.10). Retaining only the leading-order terms and assuming that $b_{\pm} \gg \gamma_a$, we find

$$\begin{aligned}
\gamma_x &\approx \frac{\gamma_a}{2} \left[1 + 2(N \pm M) \frac{b_{\pm}}{b_{\pm} + 3\gamma_a/4} \right] \\
&\approx \frac{\gamma_a}{2} [1 + 2(N \pm M)], \\
\gamma_y &\approx \frac{\gamma_a}{2}, \\
\gamma_z &\approx \gamma_a \left[1 + (N \pm M) \frac{b_{\pm}}{b_{\pm} + \gamma_a/2} \right] \\
&\approx \gamma_a [1 + (N \pm M)],
\end{aligned} \tag{3.11}$$

and

$$\Omega_z \approx \Omega_y \approx \Omega_0. \tag{3.12}$$

For large squeezing ($N \gg 1$), we have

$$\begin{aligned}
N - M &\approx -\frac{1}{2} + \frac{1}{8N}, \\
N + M &\approx 2N + \frac{1}{2}.
\end{aligned} \tag{3.13}$$

Hence, as we alter the phase ϕ_0 , the decay rates γ_x and γ_z may be enlarged or reduced compared to their normal-vacuum values. In particular (for $N \gg 1$), we note the following.

(i) The component $\langle S_x(t) \rangle$ decays at an enhanced rate $\gamma_x \approx 2N\gamma_a$ for $\phi_0 = 0$ and at an inhibited rate $\gamma_x \approx \gamma_a/8N$ for $\phi_0 = \pi/2$. The decay rate γ_x gives the width of the central peak observed in the resonance fluorescence spectrum (Mollow triplet), and hence we predict a phase-sensitive central peak width, varying between supernatural and subnatural values. The maximum reduction in

width may in principle approach 100%.

(ii) The components $\langle S_y(t) \rangle$ and $\langle S_z(t) \rangle$ decay at the enhanced rate $\frac{1}{2}(\gamma_y + \gamma_z) \approx \gamma_a N$ for $\phi_0 = 0$ and at the inhibited rate $\frac{1}{2}(\gamma_y + \gamma_z) \approx (3\gamma_a/4)(\frac{2}{3} + 1/12N)$ for $\phi_0 = \pi/2$. This decay rate corresponds to the width of the Rabi sidebands in the fluorescence triplet. Hence the sidebands should exhibit a phase sensitivity similar to that shown by the central peak, but with smaller enhancement and reduction of the linewidth.

For the choice of phase $\phi_0 = 0$, the results for γ_x and $\frac{1}{2}(\gamma_y + \gamma_z)$ are identical to those found in the "single-mode" white-noise limit. However, for $\phi_0 = \pi/2$ an important difference is apparent. The "two-mode" squeezed-vacuum result predicts a value for $\frac{1}{2}(\gamma_y + \gamma_z)$ that is much less than its white-noise counterpart, and which may in fact be less than its normal-vacuum value. Hence it is possible for all three peaks in the fluorescence triplet to exhibit subnatural linewidths for a particular choice of phase. In the white-noise treatment, line narrowing is seen only in the central fluorescence peak, while in the narrow-bandwidth treatment of Ref. 1, line narrowing occurs predominantly in the Rabi sidebands. Hence the "two-mode" squeezing scheme offers an advantage in terms of line narrowing and resolution of spectral peaks.

B. Solution via stochastic simulation

The presence of non-white-noise sources in the stochastic equations makes it impossible to obtain exact analytical solutions, and so for a more accurate description of the dynamics than that given in Sec. III A, we turn to numerical simulation. Our approach is the same as that used in Ref. 1, but for completeness we shall outline the essential features of the method.

Equations (3.3) are simulated using a fully implicit numerical integration scheme.⁸ This scheme approximates the equations with the form

$$\Delta \mathbf{S}^n = \mathbf{S}^{n+1} - \mathbf{S}^n = \mathbf{A}(\mathbf{S}^{n+\theta_1}) \Delta t + \mathbf{B}(\mathbf{S}^{n+\theta_2}) \beta_X^{c,n} \Delta t + \mathbf{C}(\mathbf{S}^{n+\theta_2}) \beta_Y^{c,n} \Delta t, \quad (3.14)$$

where

$$\mathbf{S} = \begin{pmatrix} \bar{S}_x \\ \bar{S}_y \\ \bar{S}_z \end{pmatrix}, \quad (3.15)$$

$$\mathbf{A}(\mathbf{S}) = \begin{pmatrix} -(\gamma_a/2)\bar{S}_x - \Delta_a \bar{S}_y \\ -(\gamma_a/2)\bar{S}_y + \Delta_a \bar{S}_x - \Omega_0 \bar{S}_z \\ -\gamma_a - \gamma_a \bar{S}_z + \Omega_0 \bar{S}_y \end{pmatrix},$$

$$\mathbf{B}(\mathbf{S}) = \begin{pmatrix} -\bar{S}_z \\ 0 \\ \bar{S}_x \end{pmatrix}, \quad (3.16)$$

$$\mathbf{C}(\mathbf{S}) = \begin{pmatrix} 0 \\ -\bar{S}_z \\ \bar{S}_y \end{pmatrix},$$

Δt is the timestep, $\theta_1, \theta_2 \in [0, 1]$, and

$$\mathbf{A}(\mathbf{S}^{n+\theta_1}) = \mathbf{A}(\mathbf{S}^n) + \underline{\mathbf{J}}_A^n \theta_1 \Delta \mathbf{S}^n, \quad (\underline{\mathbf{J}}_A^n)_{ij} = \left. \frac{\partial A_i}{\partial S_j} \right|_{\mathbf{S}=\mathbf{S}^n} \quad (3.17)$$

$$\mathbf{B}(\mathbf{S}^{n+\theta_2}) = \mathbf{B}(\mathbf{S}^n) + \underline{\mathbf{J}}_B^n \theta_2 \Delta \mathbf{S}^n, \quad (\underline{\mathbf{J}}_B^n)_{ij} = \left. \frac{\partial B_i}{\partial S_j} \right|_{\mathbf{S}=\mathbf{S}^n} \quad (3.18)$$

$$\mathbf{C}(\mathbf{S}^{n+\theta_2}) = \mathbf{C}(\mathbf{S}^n) + \underline{\mathbf{J}}_C^n \theta_2 \Delta \mathbf{S}^n, \quad (\underline{\mathbf{J}}_C^n)_{ij} = \left. \frac{\partial C_i}{\partial S_j} \right|_{\mathbf{S}=\mathbf{S}^n},$$

(i.e., we linearize about the point \mathbf{S}^n). It is straightforward to show that

$$\underline{\mathbf{J}}_A^n = \begin{bmatrix} -\gamma_a/2 & -\Delta_a & 0 \\ \Delta_a & -\gamma_a/2 & -\Omega_0 \\ 0 & \Omega_0 & -\gamma_a \end{bmatrix},$$

$$\underline{\mathbf{J}}_B^n = \begin{bmatrix} 0 & 0 & -1 \\ 0 & 0 & 0 \\ 1 & 0 & 0 \end{bmatrix}, \quad (3.19)$$

$$\underline{\mathbf{J}}_C^n = \begin{bmatrix} 0 & 0 & 0 \\ 0 & 0 & -1 \\ 0 & 1 & 0 \end{bmatrix}.$$

Substitution of (3.17) and (3.18) into (3.14) leads to the integration scheme

$$\Delta \mathbf{S}^n = (1 - \theta_1 \underline{\mathbf{J}}_A^n \Delta t - \theta_2 \underline{\mathbf{J}}_B^n \beta_X^{c,n} \Delta t - \theta_2 \underline{\mathbf{J}}_C^n \beta_Y^{c,n} \Delta t)^{-1} \times [\mathbf{A}(\mathbf{S}^n) \Delta t + \mathbf{B}(\mathbf{S}^n) \beta_X^{c,n} \Delta t + \mathbf{C}(\mathbf{S}^n) \beta_Y^{c,n} \Delta t]. \quad (3.20)$$

The choice $\theta_1 = \theta_2 = 0$ corresponds to the Euler method of integration. This method, however, can suffer stability problems, especially when large Rabi frequencies are involved. Hence we adopt the time-centered scheme $\theta_1 = \theta_2 = \frac{1}{2}$ (fully implicit method), which has very good stability properties.

Noise sources with the correct statistics are constructed using summations of suitably weighted Gaussian distributed random numbers. The negative correlations that characterize squeezing require that these sources be complex. This enables $\bar{S}_x(t)$, $\bar{S}_y(t)$, and $\bar{S}_z(t)$ to develop imaginary parts, but in practice these average to zero after a sufficient number of trials, provided that the integration routine is stable.

1. Results for the spin averages

Our first set of results are obtained for parameters that should roughly satisfy the conditions of the decorrelation approximation ($\Omega_0 \gg b_{\pm} \gg \gamma_a$). In Fig. 1 the squeezing parameters correspond to a 64% reduction in noise (below the vacuum level) at the frequencies $\pm \delta_c$. This reduction in fluctuations extends over a bandwidth $2b_- = 12.5\gamma_a$.

As predicted by the decorrelation approximation,

$\langle S_x(t) \rangle$ and $\langle S_z(t) \rangle$ exhibit enhanced decay rates for $\phi_0=0$ and reduced decay rates for $\phi_0=\pi/2$. The simultaneous inhibition of the decay of $\langle S_x(t) \rangle$ and $\langle S_z(t) \rangle$ is perhaps the most significant feature of the “two-mode” squeezed-vacuum scheme. This feature is more dramatically demonstrated in Fig. 2, where the maximum squeezing has been increased to 89%.

It is interesting to compare decay rates obtained from the simulations and from the decorrelation approximation. An exponential fit to the curves of Figs. 1(b) and 1(c) yields decay rates $\gamma_x \approx 1.4\gamma_a$, $(\gamma_y + \gamma_z)/2 \approx 1.2\gamma_a$ for $\phi_0=0$, and $\gamma_x \approx 0.20\gamma_a$, $(\gamma_y + \gamma_z)/2 \approx 0.60\gamma_a$ for $\phi_0=\pi/2$. In comparison result (3.11) gives

$$\begin{aligned} \gamma_x &\approx \frac{\gamma_a}{2} \left[1 + 2(N \pm M) \frac{b_{\pm}}{b_{\pm} + 3\gamma_a/4} \right] \\ &= 1.2\gamma_a, 0.21\gamma_a, \\ \frac{1}{2}(\gamma_y + \gamma_z) &\approx \frac{\gamma_a}{2} \left[\frac{3}{2} + (N \pm M) \frac{b_{\pm}}{b_{\pm} + \gamma_a/2} \right] \\ &= 1.1\gamma_a, 0.60\gamma_a, \end{aligned}$$

for $\phi_0=0$ and $\pi/2$, respectively. This level of agreement does not persist as the bandwidths b_{\pm} are reduced, highlighting the limitations of the decorrelation approxi-

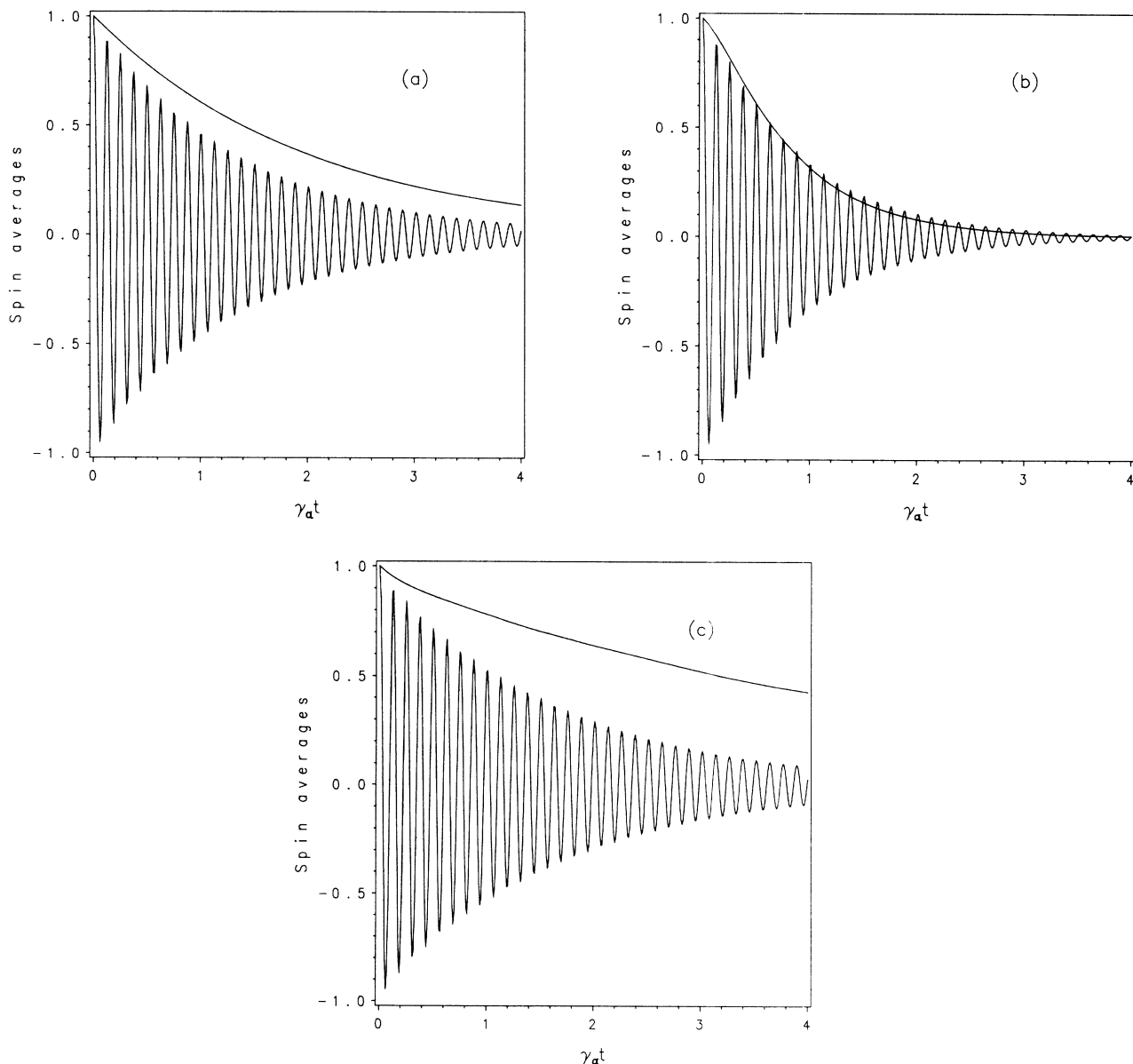


FIG. 1. Spin averages $\langle S_x(t) \rangle$ and $\langle S_z(t) \rangle$ (oscillating) computed by simulation (5000 trials) for $\Omega_0=50\gamma_a$, $\Delta_a=0$, $\delta_c=50\gamma_a$, and $\gamma_c=10\gamma_a$, with (a) $\epsilon_c=0$ (no squeezing), (b) $\epsilon_c=2.5\gamma_a$ (64% maximum squeezing), $\phi_0=0$, and (c) $\epsilon_c=2.5\gamma_a$, $\phi_0=\pi/2$.

mation. However, the basic predictions of Sec. III A are confirmed.

2. Correlation functions and spectra

The spin averages give us a good insight into the behavior of the atomic system, but for connections to be made with observable quantities such as the fluorescence spectrum, we must compute correlation functions. Methods for computing correlation functions from the adjoint equation have been outlined in Ref. 7 and were used in Ref. 1. Briefly, if the solutions of the equations of motion (3.3) are written in the form

$$\bar{S}_i(t) = \sum_j f_{ij}(t, t') \bar{S}_j(t') + g_i(t, t'), \quad (3.21)$$

then the stationary correlation functions are given by

$$\begin{aligned} \langle S_i(t) S_k(t') \rangle &= \langle f_{ik}(t, t') \rangle + \langle g_i(t, t') g_k^{st}(t') \rangle \\ &+ i \sum_{l, m} \epsilon_{lkm} \langle f_{il}(t, t') g_m^{st}(t') \rangle, \end{aligned} \quad (3.22)$$

where $g_i(t, t') \rightarrow g_i^{st}(t)$ as $t \rightarrow \infty$.

Expression (3.22) is evaluated from stochastic simulation as follows. We first allow the equations to evolve to a stationary state, thereby obtaining a value for $g_i^{st}(t')$. A new trajectory is then initiated, with four different sets of initial conditions, so that we may identify $f_{ij}(t, t')$ and $g_i(t, t')$. The procedure is then repeated, and after a suitable number of trials, the average is taken. We remove the coherent contribution to the correlation functions and sample to a time at which the correlation functions are small (so as to avoid aliasing in the fast-Fourier transform).

A major consideration in the computation of output spectra from systems subjected to squeezed light is the effect of reflections of the input squeezed light.^{7,9} One must allow not only for the nonzero power spectrum of the squeezed vacuum, but also for correlations that are established between the reflected squeezed light and light radiated from the system. These correlations can substantially affect the total fluorescence spectrum.

Using our formalism, it is relatively straightforward to incorporate reflections of the input squeezed vacuum in the output. The basic formula relating the output field to input and atomic fields has the simple form

$$E_{\text{out}}(t) = E_{\text{in}}(t) - i\sqrt{\gamma_a \hbar \omega_a} [S^-(t) - S^+(t)], \quad (3.23)$$

with which we can develop expressions for the correlation functions of the total output field. These expressions can then be computed numerically from the simulations in a straightforward manner. The fluorescence spectrum including reflections is given by the Fourier transform of the correlation function $\langle E_{\text{out}}^{(-)}(t) E_{\text{out}}^{(+)}(0) \rangle$. In this fluorescence spectrum the squeezed-vacuum power spectrum contributes peaks at the frequencies $\omega_0 \pm \delta_c$. In general, these peaks dominate the much smaller Rabi sidebands that appear at the same frequencies ($\Omega_0 = \delta_c$, $\Delta_a = 0$). However, the central atomic fluorescence peak, which is well separated from the sidebands, is essentially unaffected by the inclusion of reflections, and so the most significant line narrowing and broadening is still clearly visible in the spectrum.

We shall concentrate here on the fluorescence spectrum without reflections included. This is computed by Fourier transforming the correlation function $\langle S^+(t) S^-(0) \rangle$ and corresponds to observing the light radiated from the atom through a small "window" of unsqueezed-vacuum modes. In a cavity configuration (in which the squeezed light is incident on the atom through the cavity modes), this is equivalent to observing the fluorescence out the side of the cavity.

To begin, we compute the fluorescence spectrum for the parameters used in Fig. 1. The results are displayed

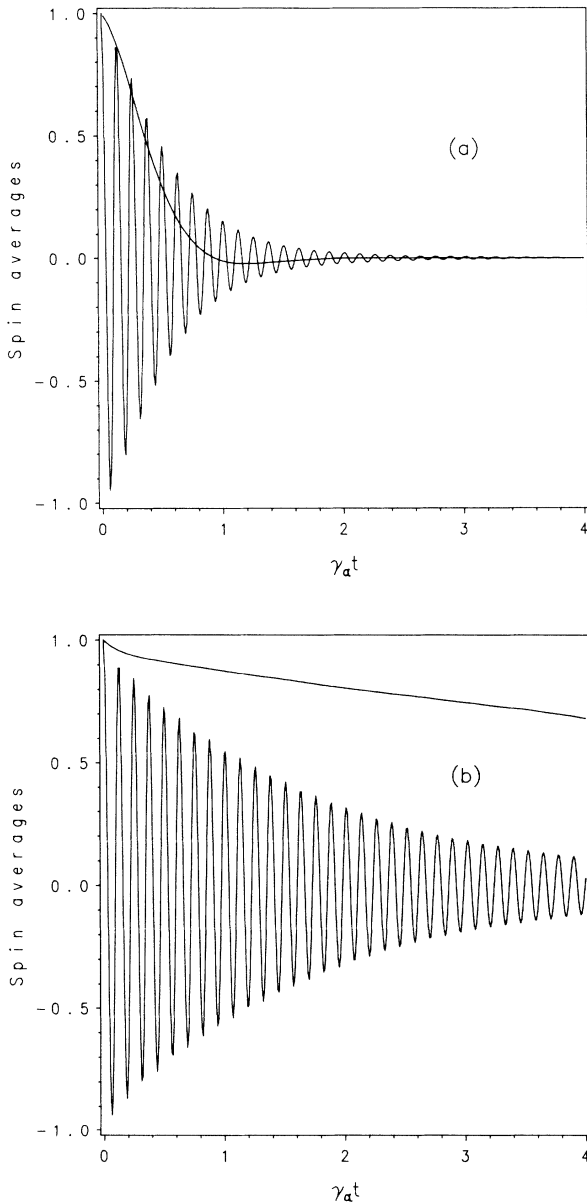


FIG. 2. Spin averages $\langle S_x(t) \rangle$ and $\langle S_z(t) \rangle$ (oscillating) computed by simulation (5000 trials) for $\Omega_0 = 50\gamma_a$, $\Delta_a = 0$, $\delta_c = 50\gamma_a$, and $\gamma_c = 10\gamma_a$, with (a) $\epsilon_c = 5.0\gamma_a$ (89% maximum squeezing), $\phi_0 = 0$, and (b) $\epsilon_c = 5.0\gamma_a$, $\phi_0 = \pi/2$.

in Fig. 3, and they confirm earlier predictions regarding narrowing and broadening of the spectral peaks. For $\phi_0=0$, all three peaks are broadened, while for $\phi_0=\pi/2$, all three peaks exhibit some degree of narrowing compared to their ordinary vacuum profiles. Although the extent of narrowing in the sidebands is modest (remember we are considering an input with only 64% maximum squeezing), it is important to note the contrast with the “single-mode” white-noise squeezing model,² which, for the same amount of squeezing, yields sidebands with significantly broadened linewidths. With increased levels

of squeezing, more substantial narrowing of the sidebands occurs in the two-mode model, and the contrast is even more pronounced. We note that the linewidths observed in the fluorescence spectra of Fig. 3 are in good agreement with the decay rates exhibited by the simple spin averages in Fig. 1.

For completeness and to highlight the points made earlier regarding reflections, we display in Fig. 4 the fluorescence spectrum with reflections of the squeezed input included. The spectra obtained with reflections included are inherently more noisy than the simple atomic fluores-

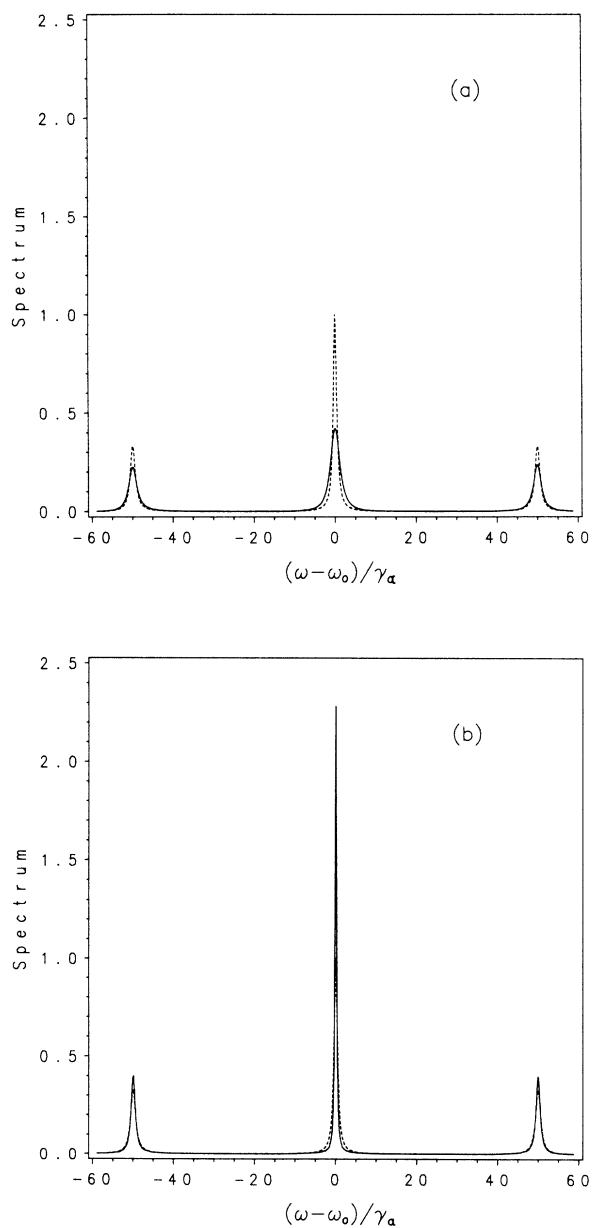


FIG. 3. Fluorescence spectrum, omitting reflections [i.e., Fourier transform of $\langle S^+(t)S^-(0) \rangle$], computed by simulation (20 000 trials) for the parameters of Fig. 1 with (a) $\phi_0=0$ and (b) $\phi_0=\pi/2$. The dashed curve in each figure is the ordinary vacuum spectrum.

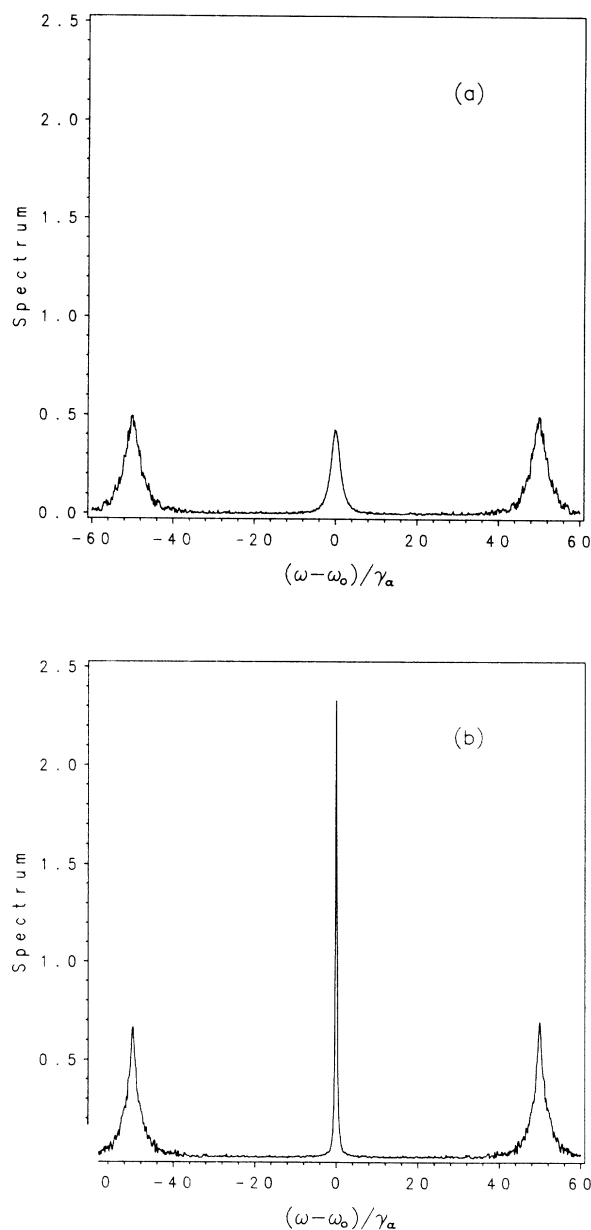


FIG. 4. Fluorescence spectrum, including reflections [i.e., Fourier transform of $\langle E_{\text{out}}^{(-)}(t)E_{\text{out}}^{(+)}(0) \rangle$], computed by simulation (20 000 trials) for the parameters of Fig. 1 with (a) $\phi_0=0$ and (b) $\phi_0=\pi/2$.

cence spectra. This can, of course, be alleviated by averaging over a greater number of trials.

It is a worthwhile exercise to gauge the extent to which the effects of line narrowing and broadening persist for values of the parameters that do not strictly satisfy the conditions upon which earlier predictions were made. This may be well be a problem facing any realistic experiment. We consider the case in which the squeezed-vacuum bandwidth is only of the order of the atomic linewidth (i.e., $b_{\pm} \sim \gamma_a$), and in addition, we reduce the Rabi frequency to the value $\Omega_0 = 20\gamma_a$. The fluorescence spectra are shown in Fig. 5. As one might expect, the extent of line narrowing and broadening is somewhat re-

duced compared to the results obtained under more ideal conditions, as in Fig. 3. However, the effects are still plainly visible, which together with other results we have gathered, enables us to conclude that the basic predictions of Sec. III A are reasonably robust in the face of nonideal inputs.

Finally, we allow for a nonzero laser-atom detuning ($\Delta_a \neq 0$). In view of the unusual spectrum of noise experienced by the atom, we might expect some interesting phenomena, especially when $\Omega_0^2 + \Delta_a^2 = \delta_c^2$. This is indeed the case, as we demonstrate in Fig. 6. It is clear that the response of the zero-frequency and oscillating components of the Bloch vector to the squeezed noise allows

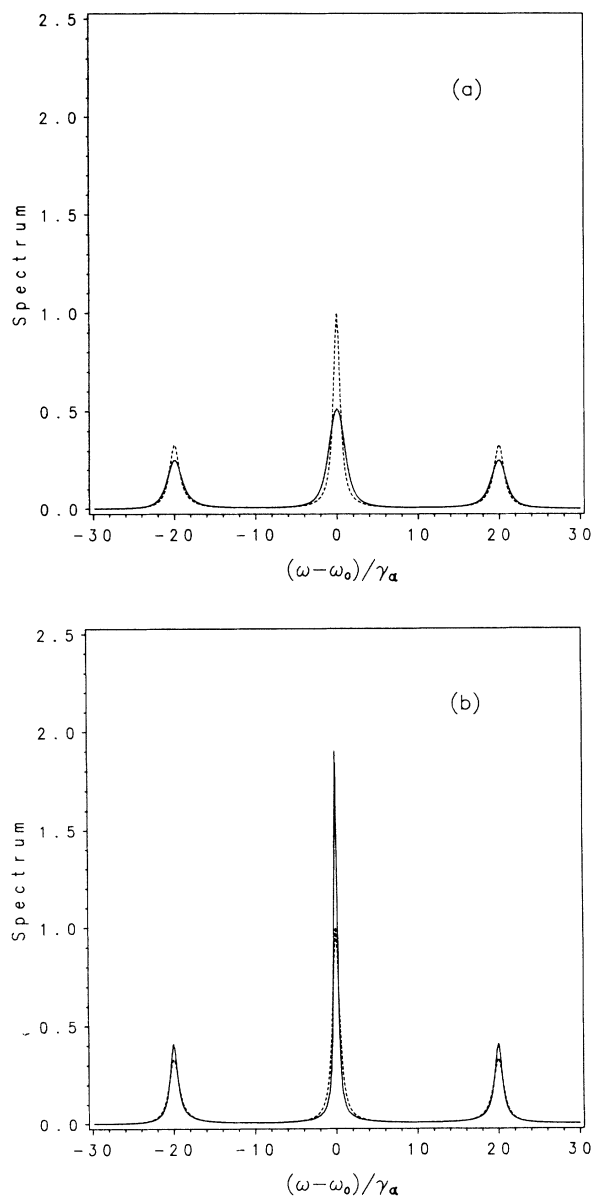


FIG. 5. Fluorescence spectrum, omitting reflections, computed by simulation (8000 trials) for $\Omega_0 = 20\gamma_a$, $\Delta_a = 0$, $\delta_c = 20\gamma_a$, $\gamma_c = 2\gamma_a$, and $\epsilon_c = 0.6\gamma_a$ (71% maximum squeezing), with (a) $\phi_0 = 0$ and (b) $\phi_0 = \pi/2$. The dashed curve in each figure is the ordinary vacuum spectrum.

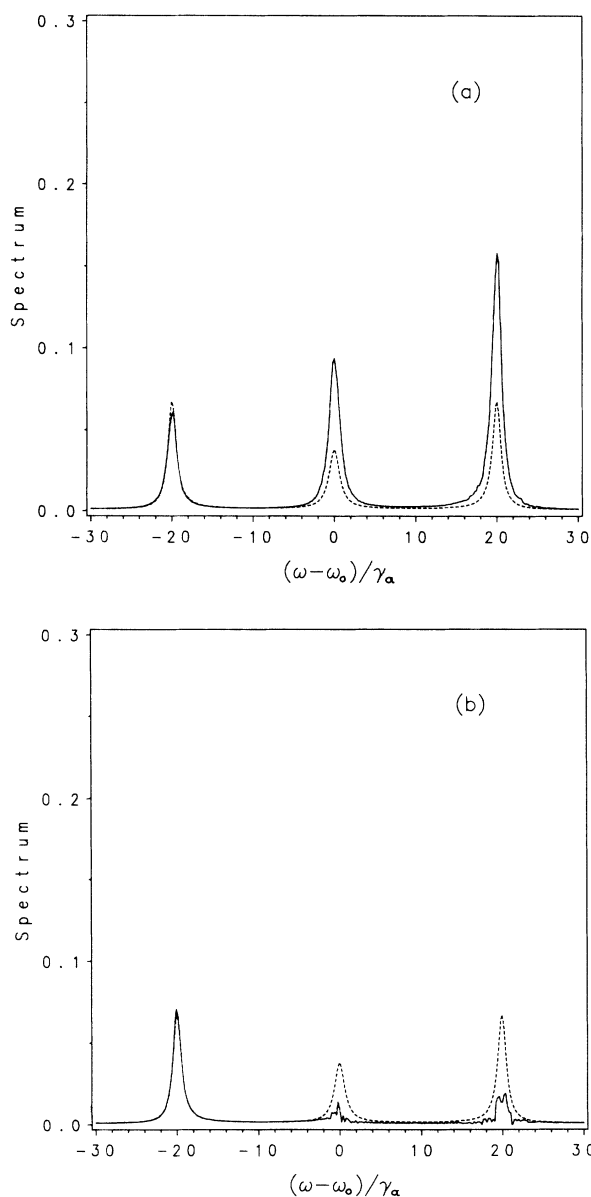


FIG. 6. Fluorescence spectrum, omitting reflections, computed by simulation (20 000 trials) for $\Omega_0 = 14.14\gamma_a$, $\Delta_a = 14.14\gamma_a$, $\delta_c = 20\gamma_a$, $\gamma_c = 2\gamma_a$, and $\epsilon_c = 0.173\gamma_a$ (29% maximum squeezing), with (a) $\phi_0 = 0$ and (b) $\phi_0 = \pi/2$. The dashed curve in each figure is the ordinary vacuum spectrum.

for a significant modification of the ordinary fluorescence spectrum. The asymmetry in the spectrum, and the enhancement or suppression of peaks (to an extent that is dependent also on the phase ϕ_0), is quite dramatic and suggests alternative signatures one might look for in detecting squeezed light. Similar effects have been seen in analyses of the interaction of (single-mode) broadband squeezed light with two-level atoms^{10,11} and have been described in terms of dressed-state population trapping.¹⁰ The parameters of Fig. 6 have been chosen after consideration of approximate analytical results, which predict strong enhancement and suppression of two peaks for suitable choices of detuning, squeezing, and phase. It is interesting to note the relatively small amount of squeezing required to produce significant effects.

IV. CONCLUSION

In Ref. 1 it was shown that narrow-bandwidth squeezed light offers interesting new possibilities in the field of squeezed-light spectroscopy. In this paper we have continued with this theme, extending the earlier work to treat a “two-mode” squeezed-vacuum input. Resonance fluorescence of a two-level atom is a particularly suitable problem to analyze as the Rabi frequency provides a control over which spectral components of the reservoir contribute to Bloch-vector damping. Using this fact, the atom can be “tuned” to the spectral peaks of the two-mode squeezed vacuum, and as we have seen, this leads to the characteristic line narrowing and broadening found in previous “single-mode” squeezing analyses. However, in the single-mode broadband squeezing analysis, the atom “sees” enhanced vacuum fluctuations at frequency ω_0 due to the noisy quadrature. In the two-mode formulation, in which the spectral peaks of the squeezed vacuum are well separated at the frequencies $\omega_0 \pm \delta_c$, the atom “sees” only ordinary vacuum fluctuations at frequency ω_0 . This means that broadening need

not occur in the fluorescence spectrum, and in fact, it is possible for all three lines in the fluorescence triplet to exhibit subnatural linewidths. Hence a variation on the narrow-bandwidth problem considered in Ref. 1 has been shown to offer still further possibilities for squeezed-light spectroscopy.

Any experimental attempt to observe these effects is likely to employ a cavity with injected squeezed light to effect a suitable squeezed-vacuum—atom coupling. The particular model we have discussed here corresponds to a cavity operating in the low- Q limit.

The assumption that the atom couples only to squeezed modes of the radiation field also requires that the decay of the atom into the cavity modes is substantially greater than decay through any other channels (e.g., out the sides of the cavity). This could be achieved, as suggested by Parkins and Gardiner,¹² by using a microcavity (i.e., plane mirrors separated by half a wavelength) with a suitably mode-matched injected squeezed vacuum. In this configuration, reflections of the input squeezed light would be inevitable in the observed output spectra.

Alternatively, one might consider the (macroscopic) confocal optical cavities used in demonstrations of cavity-enhanced spontaneous emission.¹³ For this case reflections of the input could be avoided by observing the light emitted out the sides of the cavity. Provided the enhanced spontaneous emission rate into the cavity modes is at least comparable to the free-space decay rate, significant effects should be visible in the fluorescent light.

ACKNOWLEDGMENTS

I would like to thank Dr. Barry Sanders, Dr. Margaret Reid, and Professor Crispin Gardiner for helpful comments and discussions. This work was supported by the New Zealand University Grants Committee.

¹A. S. Parkins, *Phys. Rev. A* **42**, 4352 (1990).

²H. J. Carmichael, A. S. Lane, and D. F. Walls, *Phys. Rev. Lett.* **58**, 2539 (1987); *J. Mod. Opt.* **34**, 821 (1987).

³M. Lewenstein and T. W. Mossberg, *Phys. Rev. A* **37**, 2048 (1988); M. Lewenstein, T. W. Mossberg, and R. J. Glauber, *Phys. Rev. Lett.* **59**, 775 (1987).

⁴M. J. Collett, R. Loudon, and C. W. Gardiner, *J. Mod. Opt.* **34**, 821 (1987).

⁵M. D. Reid and P. D. Drummond, *Phys. Rev. A* **41**, 3930 (1990).

⁶M. G. Raizen, L. A. Orozco, M. Xiao, T. L. Boyd, and H. J. Kimble, *Phys. Rev. Lett.* **59**, 198 (1987); L. A. Orozco, M. G. Raizen, M. Xiao, R. J. Brecha, and H. J. Kimble, *J. Opt. Soc. Am. B* **4**, 1490 (1987).

⁷A. S. Parkins and C. W. Gardiner, *Phys. Rev. A* **37**, 3867 (1988).

⁸K. J. McNeil and I. J. D. Craig, *Phys. Rev. A* **41**, 4009 (1990); A. M. Smith and C. W. Gardiner, *ibid.* **39**, 3511 (1989).

⁹C. W. Gardiner, A. S. Parkins, and M. J. Collett, *J. Opt. Soc. Am. B* **4**, 1683 (1987).

¹⁰J.-M. Courty and S. Reynaud, *Europhys. Lett.* **10**, 237 (1989).

¹¹T. A. B. Kennedy and D. F. Walls, *Phys. Rev. A* **42**, 3051 (1990).

¹²A. S. Parkins and C. W. Gardiner, *Phys. Rev. A* **40**, 3796 (1989); **42**, 5765(E) (1990).

¹³D. J. Heinzen, J. J. Childs, J. E. Thomas, and M. S. Feld, *Phys. Rev. Lett.* **58**, 1320 (1987).